Physics Letters B 675 (2009) 415–419

Contents lists available at ScienceDirect

Physics Letters B

www.elsevier.com/locate/physletb

Oscillations in radioactive exponential decay

T.M. Semkow [a,*], D.K. Haines [a], S.E. Beach [a], B.J. Kilpatrick [a], A.J. Khan [a], K. O'Brien [b]

[a] Wadsworth Center, New York State Department of Health, Albany, NY 12201, USA
[b] Department of Physics and Astronomy, Northern Arizona University, Flagstaff, AZ 86011, USA

ARTICLE INFO

Article history:
Received 19 February 2009
Received in revised form 2 April 2009
Accepted 19 April 2009
Available online 22 April 2009
Editor: V. Metag

PACS:
23.40.-s
23.20.-g
24.80.-y
29.40.Cs

Keywords:
Quantum state decay
Ionization chamber
Proportional counter
Beta decay
Gamma decay
Energy loss

ABSTRACT

Several older and recent reports provided evidence for the oscillatory character of the exponential decay law in radioactive decay and attempted to explain it with basic physics. We show here that the measured effects observed in some of the cases, namely in the decay of ^{226}Ra, ^{32}Si in equilibrium, and ^{36}Cl, can be explained with the temperature variations.

1. Introduction

Exponential decay law is expressed as the quantum-mechanical probability of survival of a single atom in time t, $e^{-\lambda t}$, where λ is the decay constant, which is equal to the ratio of the average number of atoms that survived the decay to the original number of atoms. The exponential decay law has been satisfied in nuclear systems, whereas evidence exists for deviations from it in atomic systems (see Ref. [1] for a review). Studying exponential decay is fundamentally important since it provides an insight to the decay of quantum state. Exponential decay has wide applications in several fields as it is used for quantification of radionuclides.

Several investigations revealed fluctuations superimposed on average exponential decay curves, which can be seen as clear oscillations in many systems. Alburger et al. measured the decay of ^{32}Si and ^{36}Cl on a gas proportional counter [2]. Both decay curves have showed oscillations superimposed on them with a period of 1 year and a phase shift of approximately 1 month. The maximum occurred in the summer and the minimum in winter. In addition, a ratio ^{32}Si/^{36}Cl was calculated, in which the oscillations are reversed, i.e., they exhibit maximum in winter and minimum in the summer. The relative amplitudes (relative peak-to-valley deviations) of the counting rates were between 1.5×10^{-3} and 3×10^{-3}. The radioactive decay curves for ^{226}Ra and daughters that had been measured in an ionization chamber by Siegert et al., reveal oscillations of similar amplitude, with the maximum in the winter and minimum in the summer [3]. Jenkins et al. correlated the ^{32}Si/^{36}Cl and ^{226}Ra oscillations with the distance between the Earth and the Sun (the shorter the distance in winter, the higher the decay rate measured) [4]. This correlation led them to two possible explanations: solar scalar field modification of the fine structure constant and thus the decay rates or neutrino flux from the Sun interacting with the radioactive nuclei in a novel way. Seasonal oscillations are also seen in the decay of ^{152}Eu measured on a Ge(Li) γ-ray spectrometer by [3].

Godovikov measured the decays of two Mössbauer sources: ^{119m}Sn and ^{125m}Te using a NaI detector [5,6]. It is remarkable that both measurements revealed seasonal oscillations with the same period of 1 y and the same phase shift with maximum in the summer and minimum in the winter. They resemble the seasonal variations for the proportional detector or ionization chamber data [2,3], with the exception of the relative amplitudes be-

* Corresponding author. Tel.: +1 518 474 6071; fax: +1 518 473 6950.
E-mail address: tms15@health.state.ny.us (T.M. Semkow).

0370-2693/$ – see front matter
doi:10.1016/j.physletb.2009.04.051

ing much higher (between 0.093 and 0.17). These results were explained by the author with the multiple absorptions and reemissions of γ quanta in the stable Sn and Te nuclei of the source. This was hypothesized as a collective nuclear system in which individual decay events were no longer spontaneous, and thus leading to the oscillations. Opalenko et al. suggested that the oscillations could be caused by instability in the detection system and a narrow discriminator window for the Mössbauer measurements [7].

Litvinov et al. observed oscillations with a period of about 7 s superimposed on the electron capture (EC) decay curves for highly ionized, hydrogen-like ^{140}Pr and ^{142}Pm [8]. The ions were produced by projectile fragmentation and fragment separation at the GSI Darmstadt accelerator, followed by an injection into a cooler-storage ring. The EC decay was detected by change of the ion evolution frequency due to a different mass of the daughter nucleus. Litvinov et al. proposed that the oscillations were caused by energy splitting due to two neutrino mass eigenstates. However, the oscillations were not confirmed for ^{142}Pm, in an experiment by Vetter et al. consisting of a more traditional counting of X rays from the ^{142}Nd daughter [9].

The proposed explanations for the oscillations invoke basic physics and astrophysics. It is, therefore, important to carefully evaluate the data and evidence provided. The purpose of the present Letter is to reanalyze the data by Alburger et al. and Siegert et al., leading to alternative explanations of the oscillations in exponential decay.

2. Ionization chamber data

Siegert et al. reported a nearly 12-y decay data for the ^{226}Ra ($T_{1/2} = 1600$ y) comparison source in conjunction with the half-life measurements of Eu isotopes [3]. Jenkins et al. obtained the original data, extended up to 15 years, from those authors [4]. The background-corrected data exhibit periodic oscillations about a fitted exponential decay with relative amplitude (relative peak-to-valley deviations) of the counting rate $\delta C = 3 \times 10^{-3}$. Siegert et al. suggested that the oscillations could be caused by a discharge on the ionization chamber electrode due to radon daughters in the air, which show seasonal variations. Such oscillations could also be due to background, humidity, or temperature variations.

The ionization-chamber measurement is characterized by a high counting rate from the radium source and a small background. There is no information about the value of background [3], so possible oscillations due to background cannot be evaluated for these data. The humidity could affect the density of the gas in the ionization chamber. However, since the chamber constitutes a closed system, no ambient seasonal humidity variations would affect the gas inside the chamber. Such humidity variations, similarly to the radon daughters, could affect any possible discharge on the electrode.

We have observed gain shifts due to temperature variations in ionization chamber experiments in our laboratory [10]. The effect of temperature on the oscillations can be easily estimated using principles of radiation interaction. The ionization chamber used by Siegert et al. consisted of a 32-cm high cylinder with a 5-cm diameter well for insertion of the source and a 7.2-cm radial length [11]. It was pressurized with argon to $p = 20$ atm (2 MPa). The ^{226}Ra source, in equilibrium with the daughters, was encapsulated in a stainless steel tube. Therefore, γ radiations from the radium daughters were detected in the ionization chamber.

Since the chamber operated at a constant pressure, it follows that $\rho T = \text{const}$, where ρ is the gas density and T an absolute temperature, according to the ideal gas law. Therefore, a small relative temperature change $\delta T = |\Delta T/T|$ changes the relative gas density $\delta\rho = |-\Delta\rho/\rho|$, such that $\delta\rho = \delta T$. The increase of gas density causes greater γ-ray attenuation and, consequently, a higher counting rate. It can be shown that the relative counting rate change $\delta C = |\Delta C/C|$ in the detector due to this effect is given by

$$\delta C = \frac{e^{-\mu\rho x}}{1 - e^{-\mu\rho x}} \mu\rho x \delta T, \tag{1}$$

where μ is an average γ-ray attenuation coefficient and x is the average length of the radiation path in the chamber.

We calculated $\mu = 0.07703$ cm^2 g^{-1} in argon using major γ rays from ^{214}Pb and ^{214}Bi [12] and their attenuation coefficients [13]. From the gas law, $\rho/p = \text{const}$, which results in $\rho = 0.03567$ g cm^{-3} for argon at the operating pressure [14]. Since the ion chamber height was greater than the radial length, we set $x = 14.4$ cm, double the radial length, as an average path of the γ rays. With these values, we calculated from Eq. (1) that the observed $\delta C = 3 \times 10^{-3}$ can be caused by $\Delta T = 0.91\,^\circ$C $= 1.6\,^\circ$F.

The above result must be considered as a lower limit. In addition to γ rays, Compton scattered photons from γ interactions in the stainless steel container will reach the ionization chamber. Also, bremsstrahlung X rays are emitted from the β particle interactions in the stainless steel container. It is difficult to calculate this effect, owing to a continuous β-energy spectrum; however, the average X-ray energy is expected to be lower than the average γ-ray energy resulting in higher μ and larger δT in Eq. (1). Nevertheless, the intensity of the X rays is expected to be lower than that of the γ rays.

Siegert et al. did not report seasonal temperature variations ΔT in their laboratory. However, it is likely that, in a temperate climate zone, the average temperature in an institutional building is higher in the summer than in the winter, if all factors such as ambient temperature, ventilation, heating, and air conditioning are taken into account.

3. Proportional detector data

Using a β gas proportional detector, Alburger et al. measured a source containing ^{32}Si ($T_{1/2} = 172$ y, $E_{\beta\,\max} = 225$ keV) [2], which decays to ^{32}P ($E_{\beta\,\max} = 1710$ keV, $T_{1/2} = 14$ d) establishing a secular equilibrium. A ^{36}Cl ($T_{1/2} = 3.0 \times 10^5$ y, $E_{\beta\,\max} = 709$ keV) comparison source was also measured. The 4-y decay data exhibit individual seasonal counting rate oscillations for the two sources, with the maximum in the summer and minimum in the winter. The ratio (^{32}Si + ^{32}P)/^{36}Cl of the normalized counting rates (abbreviated as Si/Cl) was calculated to cancel out any instrumental factors. The ratio exhibits the oscillations in an opposite direction, with the maximum in the winter and minimum in the summer. The extent of the seasonal oscillations is reproduced in Table 1. It is seen that the δC for the Si/Cl ratio, taken between maximum and minimum data points, is about 2.7×10^{-3} (rows 1 and 3), whereas an empirical fit to the data provided δC of 1.5×10^{-3} (row 2).

The ^{32}Si + ^{32}P source (abbreviated as Si) was incorporated in a SiO_2 matrix with an Al absorber on the top, for a total mass thickness of 17 mg cm^{-2} [2], which considerably limited the contribution from ^{32}Si due to self-absorption of β particles, and emphasized the contribution from ^{32}P, to the observed β counting

Table 1
Observed relative amplitudes δC of the Si and Cl counting rate oscillations.

Parameter	δC	Description	Ref.
Si/Cl	2.7×10^{-3}	max to min data	[2, Fig. 4]
Si/Cl	1.5×10^{-3}	empirical fit	[2, Fig. 4]
Si/Cl	2.8×10^{-3}	max to min data, 5 pt average	[4, Fig. 2]
Cl	4.3×10^{-3}	max to min data	[2, Fig. 3]
Si	2.8×10^{-3}	max to min data	[2, Fig. 3]
Si/Cl	1.5×10^{-3}	δC(Cl)–δC(Si)	[2, Fig. 3]

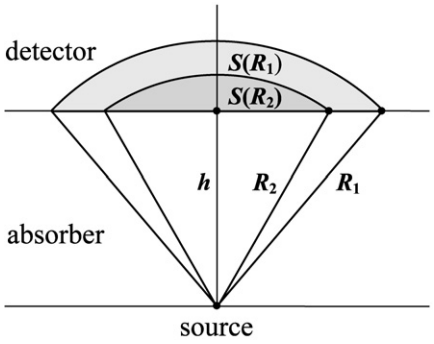

Fig. 1. Geometry of the infinite gas-proportional detector model, consisting of an absorber and the detector. Variable abbreviations: h, absorber thickness; R, β-particle range in the absorber; S, spherical cap.

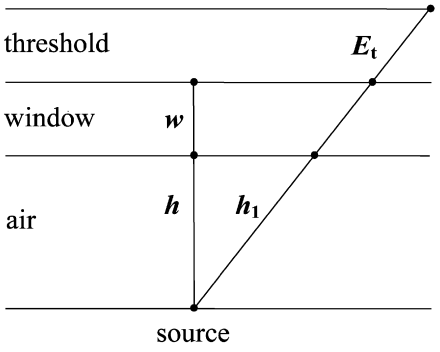

Fig. 2. Refined infinite gas-proportional detector model, consisting of air, window, and energy threshold inside the detector. Variable abbreviations: h, air thickness; w, window thickness; E_t, energy threshold.

rate from this source. Consequently, the average β energy in the Si source was higher than in the Cl source. The larger observed oscillations δC in the Cl counting rate are due to this isotope's lower β energy and thus higher sensitivity to the air-density variations, as can be compared for rows 4 and 5 in Table 1.

The oscillations can be explained with the temperature seasonal variations, since the building temperature records indicated the seasonal temperature differences within $\Delta T = 6\,^{\circ}\mathrm{F}$ (3.3 °C), and equal to 2.3 °F (1.3 °C) during the last 5 months of the experiments [2]. After emission from the source, β particles straggle through several mm of air absorber at atmospheric pressure before entering the detector chamber. To keep that pressure stable, the whole apparatus was enclosed in a box with a transducer, which maintained air pressure at 741 ± 0.5 mm Hg [15]. For constant air pressure, the air density was lower in the summer and higher in the winter, due to higher temperature in the summer. The lower density in the summer caused less β particle absorption in the air, and a higher counting rate in the detector. It should be noted that the pressure inside the pressure box had fluctuations on the order of $1/741 = 1.3 \times 10^{-3}$. However, these are random fluctuations and would not have any effect on the seasonal fluctuations of interest here.

Let us consider two oscillatory data sets, with the same periods and phases but different amplitudes. Let A_1 and A_2 are the average values of both sets, and Δ_1, Δ_2 are the peak to value amplitudes. Furthermore, let $\Delta_2/A_2 < \Delta_1/A_1 \ll 1$. Then the normalized ratio of 2/1 has oscillations in opposite direction to the individual component oscillations, with the relative amplitude

$$\frac{A_2 - \Delta_2/2}{A_2} \Big/ \frac{A_1 - \Delta_1/2}{A_1} - \frac{A_2 + \Delta_2/2}{A_2} \Big/ \frac{A_1 + \Delta_1/2}{A_1} \cong \frac{\Delta_1}{A_1} - \frac{\Delta_2}{A_2}. \tag{2}$$

Since the individual $\delta C(\mathrm{Cl}) > \delta C(\mathrm{Si})$ and both are $\ll 1$, the δC of the Si/Cl ratio is given by

$$\delta C(\mathrm{Si/Cl}) \cong \delta C(\mathrm{Cl}) - \delta C(\mathrm{Si}), \tag{3}$$

and it is listed in the last row of Table 1.

We present an approximate model of the gas-proportional detector to justify the above effects. Consider an infinite, planar gas proportional detector consisting of an absorber and the detector volume (Fig. 1). For a given β energy, the particles are counted in a solid angle subtended by a spherical cup $S(R_1)$, where R_1 is the range of β particles in the absorber. An increase in the relative absorber density $\delta\rho$ lowers the range to R_2, and the corresponding counting rate will decrease as subtended by the spherical cup $S(R_2)$. The relative decrease in the counting rate δC can be derived from the geometrical considerations in Fig. 1, and, for $\delta\rho \ll 1$, it is given by the equation below

$$\delta C = \frac{\delta\rho}{3} \frac{2 - h/R_1}{1 - h/R_1}, \tag{4}$$

where h is the absorber thickness. This equation correctly predicts that, for lower β energy (lower R_1), δC will be higher.

Next, we must incorporate the details of the absorber including air, detector window, and energy threshold for detection of β particle in the P10 gas at atmospheric pressure, as illustrated in Fig. 2. We take the mass thickness of the air $h = 0.5810$ mg cm^{-2} [2,16]. The detector window was constructed from a Kapton foil with deposited gold [15], resulting in a window mass thickness of $w = 0.8867$ mg cm^{-2}. For a given initial β particle energy E_0, the refined model is then solved for energy E at the entrance to the window, according to the equation

$$\frac{R_\mathrm{w}(E) - R_\mathrm{w}(E_\mathrm{t})}{R_\mathrm{a}(E_0) - R_\mathrm{a}(E)} = \frac{w}{h}, \tag{5}$$

where E_t is the threshold energy inside the detector. R_a and R_w are the electron ranges in air and window, respectively, interpolated from Ref. [17]. After solving Eq. (5) for E, we calculated h_1 from Fig. 2 using Eq. (6):

$$h_1 = R_\mathrm{a}(E_0) - R_\mathrm{a}(E), \tag{6}$$

followed by the calculation of $\delta C(E_0)$ from Eq. (4), with h_1 substituted for R_1.

The actual gas proportional detector differs from the model presented above due to finite size and edge effects [15,16]. The energy-loss calculations indicated that β particles deposit between 2 and 20 keV in the P10 gas of the detector, depending on the incident energy and direction, whereas the minimum β energy needed to penetrate the air and window is equal to 24 keV. Therefore, we take $E_\mathrm{t} = 2$ keV, and $E_\mathrm{et} = 26$ keV as an effective β energy threshold required for detection.

We present two calculations with our model, reproduced as rows in Table 2, where the columns contain the parameters and results. The 1st column gives the seasonal temperature differences reported by Alburger et al., from which the relative air density changes $\delta\rho$ were calculated as in Section 2 (column 2). The $\delta C(E_0)$ functions, calculated for appropriate $\delta\rho$, were numerically inte-

Table 2
Calculated relative amplitudes δC of the Si and Cl counting rate oscillations.

ΔT (°F)	$\delta\rho$	E_u (keV)	δC(Cl)	Si + P	δC(Si)	δC(Si/Cl)
2.3	4.325×10^{-3}	709	3.0×10^{-3}	0.0 + 1.0	1.5×10^{-3}	1.5×10^{-3}
6	1.127×10^{-2}	250	4.2×10^{-3}	0.15 + 0.85	2.0×10^{-3}	2.2×10^{-3}

grated over the β spectra according to Fermi theory [18], which yielded $\delta C(\mathrm{Cl})$ in column 4 and $\delta C(\mathrm{Si})$ in column 6, where Si abbreviates Si + P. The lower limit of integration was $E_{\mathrm{et}} = 26$ keV, whereas the upper integration limits E_{u} are given in column 3. Finally, $\delta C(\mathrm{Si/Cl})$ was calculated from Eq. (3) and is given in column 7.

The first calculation is for $\Delta T = 2.3\,^{\circ}\mathrm{F}$ (1st row in Table 2). The upper integration limit was set as the maximum β energy of ^{36}Cl, $E_{\mathrm{u}} = 709$ keV. For the integration of $\delta C(\mathrm{Si})$, we assumed that the Si + P source contained pure ^{32}P (column 3), reflecting the self-absorption discussed above. It is seen that the calculated $\delta C(\mathrm{Si/Cl}) = 1.5 \times 10^{-3}$ is equal to the average experimental values from Table 1, while the calculated $\delta C(\mathrm{Cl})$ and $\delta C(\mathrm{Si})$ are lower than the ones taken between the maximum and minimum data points.

The second calculation is for $\Delta T = 6\,^{\circ}\mathrm{F}$ (2nd row in Table 2). The upper integration limit was set as $E_{\mathrm{u}} = 250$ keV and the 0.15 Si + 0.85 P β spectrum was assumed. It is seen from Table 2 that the calculated $\delta C(\mathrm{Cl})$, $\delta C(\mathrm{Si})$, and $\delta C(\mathrm{Si/Cl})$ are close to the ones taken between the maximum and minimum data points from Table 1. The E_{u} integration limit reflects the fact that the real gas proportional detector has a finite radius leading to the detector edge effects. The relative contribution of Si and P reflects the self-absorption.

Alburger et al. reported also an observed seasonal relative humidity change from 35% to 75% between winter and summer. Increased humidity in the summer would increase air density which would have an opposite effect on the individual isotopes' oscillations than the temperature. We calculated $\delta\rho = 1.9 \times 10^{-4}$ between dry and moist air, under the Alburger et al. experimental conditions of 23 °C and 741 mm Hg [14]; $\delta\rho$ would be still smaller between 35% and 75% relative humidity. This value is more than one order of magnitude smaller than the $\delta\rho$ due to temperature change (Table 2), and thus less important.

It is also instructive to consider the possible effect of the seasonal environmental background fluctuations on the observed oscillations, since some of the background is dependent on the solar effects [19]. Among several components of the environmental radiation background, cosmic ray muons and radon daughters in the air are of particular relevance here.

The muon flux at the ground level is 5% lower in the summer than in the winter, since muon production layer rises in the summer, increasing the mean path to the ground [20]. The radon daughter concentration in the ambient air is typically 2 to 4 times higher in the summer than in the winter [21]. However, in residential buildings, concentration of radon and daughters are higher in winter due to the stack effect [22]. The stack effect may be less pronounced in institutional buildings due to air ventilation.

The detector counting rate $C(t)$ can be expressed as $C(t) = S(0)e^{-\lambda t} + B$, where S is the source counting rate and B is the background counting rate (not corrected for in the Alburger et al. experiment). The relative deviations from the exponential decay can be expressed as $U(t) = C(t)e^{\lambda t}/C(0)$ [4]. In $t = 4$ y duration of the experiment, $\lambda_{\mathrm{Cl}} t \ll \lambda_{\mathrm{Si}} t = 1.6 \times 10^{-2} \ll 1$. Consequently, the normalized $\delta C(\mathrm{Si/Cl})$ is given by

$$\delta C(\mathrm{Si/Cl}) = \frac{U_{\mathrm{Si}}(t)}{U_{\mathrm{Cl}}(t)} - 1 \cong \frac{B\lambda_{\mathrm{Si}} t}{C_{\mathrm{Si}}(0)}. \tag{7}$$

Substituting the experimental values $B = 6.5\ \mathrm{c\,min^{-1}}$ and $C_{\mathrm{Si}}(0) = 1.48 \times 10^4\ \mathrm{c\,min^{-1}}$, we obtain for the ratio $\delta C(\mathrm{Si/Cl}) = 7.0 \times 10^{-6}$ from Eq. (7). Therefore, the background contribution to the deviations from the exponential decay would be too small to explain the oscillations, and the background seasonal variations in muon flux and the radon daughter concentrations would be not important.

4. Germanium detector data

If the decay oscillations were caused by some influence of the Sun, they should be present in all detector systems. Siegert et al. reported also a 15-y history of detector efficiency data for a Ge(Li) γ-ray spectrometer using ^{152}Eu ($T_{1/2} = 13.5$ y) [3]. Those data appear to show some oscillations of relative amplitude $\delta C = 5.0 \times 10^{-3}$, with a period of 1 y and a phase shift of 6 months. Since the latter phase shift differs considerably from the 1-month phase shift for the ^{226}Ra data, it cannot correlate with the Earth-to-Sun distance.

5. Conclusions

Siegert et al. reported winter-summer seasonal oscillations superimposed on the radioactive decay curve of ^{226}Ra and daughters measured in the ionization chamber [3]. We have shown that the oscillations can be explained by the change of argon density in the ionization chamber. Higher summer temperatures decreased argon density, thereby lowering γ-ray absorption, which resulted in lowering of the counting rate.

Alburger et al. reported the decays of ^{32}Si + ^{32}P (abbreviated as Si) and ^{36}Cl measured in the gas proportional detector [2]. Both the Si and Cl counting rates showed winter-summer seasonal oscillations (high in the summer), while counting rate ratio Si/Cl had oscillations in the opposite direction. We have shown that these observations can be explained by the effect of the temperature on air density between the radioactive source and the detector. Higher summer temperatures decreased air density, causing less absorption of β particles in the air, resulting in higher counting rates. We have also shown that other effects such as humidity, background, muon flux, and radon concentration did not have any great effect on the seasonal oscillations of the counting rates.

The calculations presented in this work were approximate and they utilized principles of ionizing radiation interaction with matter. Despite the necessity to make several assumptions, as well as incomplete information about the original experiments, our calculations provide semi-quantitative agreement with the published data. More sophisticated detector models or Monte Carlo simulations are required for detailed study of the counting rate oscillations.

Jenkins et al. observed that the Ra and Si/Cl counting-rate oscillations correlated with the Earth-to-Sun distance (the peak of the oscillations corresponds to the shortest distance) [4]. They proposed two possible explanations: solar scalar field modification of the fine structure constant and thus the decay rates, or some novel interaction of neutrino flux from the Sun with the radioactive nuclei. While the Ra counting-rate oscillations apparently correlate with the Earth-to-Sun distance, the Si/Cl correlation is an artifact from the taking of the ratio between counting rates. The individual Si and Cl counting rates actually anti-correlate with the distance. In addition, the Eu data do not correlate with the distance.

The abovementioned original experiments by Siegert et al. and Alburger et al. were performed in the northern hemisphere in a temperate climate zone: Braunschweig, Germany, and Upton, NY, USA, respectively. Small seasonal temperature differences in institutional buildings were either estimated or could be expected, leading to the observed counting rate oscillations in different ways. Of course, the periodic oscillations of the counting rates are still caused by varying Earth–Sun distance, but not directly, only by the seasonal temperature variations resulting from the varying distance.

References

[1] T.M. Semkow, Exponential decay law and nuclear statistics, in: T.M. Semkow, S. Pommé, S.M. Jerome, D.J. Strom (Eds.), Applied Modeling and Computations

in Nuclear Science, ACS Symposium Series, vol. 945, ACS/OUP, Washington, DC, 2007, pp. 42–56.
[2] D.E. Alburger, G. Harbottle, E.F. Norton, Earth Plan. Sci. Lett. 78 (1986) 168.
[3] H. Siegert, H. Schrader, U. Schötzig, Appl. Rad. Isot. 49 (1998) 1397.
[4] J.H. Jenkins, E. Fischbach, J.B. Buncher, J.T. Gruenwald, D.E. Krause, J.J. Mattes, arXiv:0808.3283v1 [astro-ph].
[5] S.K. Godovikov, JETP Lett. 75 (2002) 499.
[6] S.K. Godovikov, JETP Lett. 79 (2004) 196.
[7] A.A. Opalenko, V.I. Vysotskii, A.A. Kornilova, JETP Lett. 79 (2004) 200.
[8] Yu.A. Litvinov, et al., Phys. Lett. B 664 (2008) 162.
[9] P.A. Vetter, et al., Phys. Lett. B 670 (2008) 196.
[10] T.M. Semkow, A.J. Khan, D.K. Haines, A. Bari, Health Phys. 96 (2009) 432.
[11] H. Schrader, Activity Measurements with Ionization Chambers, Monographie BIPM-4, Bureau International des Poids et Mesures, Sèvres, 1997.
[12] E. Browne, R.B. Firestone, Table of Radioactive Isotopes, Wiley, New York, 1986.
[13] E. Storm, H.I. Israel, Nucl. Data Tables A 7 (1970) 565.
[14] R.C. West (Ed.), CRC Handbook of Chemistry and Physics, 61 ed., CRC Press, Boca Raton, 1980.
[15] G. Harbottle, C. Koehler, R. Withnell, Rev. Sci. Instrum. 44 (1973) 55.
[16] T.M. Semkow, P.P. Parekh, Health Phys. 81 (2001) 567.
[17] ICRU Report 37, Stopping Powers for Electrons and Positrons, International Commission on Radiation Units and Measurements, Bethesda, MD, 1984.
[18] P. Marmier, E. Sheldon, Physics of Nuclei and Particles, vol. I, Academic Press, New York, 1969.
[19] K. O'Brien, A random-walk solution to the heliospheric transport equation, in: T.M. Semkow, S. Pommé, S.M. Jerome, D.J. Strom (Eds.), Applied Modeling and Computations in Nuclear Science, ACS Symposium Series, vol. 945, ACS/OUP, Washington, DC, 2007, pp. 207–216.
[20] F. Wissmann, Rad. Prot. Dos. 118 (2006) 3.
[21] J. Porstendörfer, J. Aerosol Sci. 25 (1994) 219.
[22] K.K. Nielson, V.C. Rogers, V. Rogers, R.B. Holt, Health Phys. 67 (1994) 363.